Field analysis of PAHs in surface sediments of the Pearl River Estuary and their environmental impacts

Niu, Lixia; Yang, Qingshu; van Gelder, Pieter; Zeng, Danna; Cai, Huayang; Liu, Feng

Important note
To cite this publication, please use the final published version (if applicable).
Please check the document version above.

RESEARCH ARTICLE

Field analysis of PAHs in surface sediments of the Pearl River Estuary and their environmental impacts

Lixia Niu [1,2,3] · Qingshu Yang [1,2,3] · Pieter van Gelder [4] · Danna Zeng [1] · Huayang Cai [1,2,3] · Feng Liu [1,2,3] · Xiangxin Luo [1,2,3]

Abstract

Based on a monthly field survey in 2011 of the Pearl River Estuary, the dynamics of polycyclic aromatic hydrocarbons (PAHs) in surface sediments (depth < 5 cm) were explored. The seasonal variations in PAH level and composition were investigated in this study, as well as their environmental behaviors, the role of particles, and source apportionment. The concentration of the sum of 16 priority PAHs (defined as $\sum_{16}$PAHs) ranged from 0.32 to 1.10 μg/g, while that of the sum of 62 PAHs (defined as $\sum_t$PAHs) varied from 0.83 to 2.75 μg/g. The levels of both the $\sum_{16}$PAHs and $\sum_t$PAHs peaked in February, although the minimum levels appeared in different months—December and August, respectively. The seasonal difference in the $\sum_t$PAHs was significant (flood season, 7.69 μg/g; dry season, 10.51 μg/g). The 5-ring PAH compound (e.g., perylene) was the most abundant and was responsible for 35% of the total, which implied a terrestrial input source via the Pearl River. Sediment particles were predominantly composed of clayed sand, and sediment PAHs showed a greater tendency to be adsorbed onto the large-sized particles rather than the fine fractions. Total organic carbon (TOC) could considerably facilitate the sediment PAHs. Principal component analysis revealed that vehicle emission sources, petroleum sources, and combustion sources were the major anthropogenic contamination sources. The diagnostic ratios of various individual PAHs were also explored. These findings are particularly useful for understanding the geochemistry of organic pollutants in the complex estuarine environment.

Keywords Polycyclic aromatic hydrocarbons · Surface sediments · Environmental fate · Source apportionment · Pearl River Estuary

Introduction

Polycyclic aromatic hydrocarbons (PAHs), characterized by their internal properties of carcinogenicity, toxicity, and mutagenicity, are significantly affecting the coastal marine environment and threatening human health (Valavanidis et al. 2008; Qiu et al. 2009; Moeckel et al. 2014). Numerous types of PAHs (> 100) have been detected in the environment, e.g., in air (Harrison et al. 1996; Lang et al. 2008), in water bodies (Yuan et al. 2015; Niu et al. 2018), in soils (Usman et al. 2016; Cetin 2016), and in sediments (Kannan et al. 2005; Gu et al. 2016). Of these, estuarine sediments are important pools of environmental pollutants from land (Timoney and Lee 2011; Gu et al. 2016). PAHs enter the environment via several pathways, e.g., atmospheric PAHs via deposition, terrestrial PAHs via riverine runoff, and PAHs in the water column via adsorption and desorption (Yuan et al. 2015). The final destination of PAHs is their accumulation in sediments (Mai et al. 2003). Furthermore, the geochemical behavior of PAHs in surface sediments has important implications for understanding the sink and source of organic pollutants in the complex estuarine environment.

Estuaries act as filters that trap both natural and anthropogenic materials transferred from the continents to the pelagic

Lixia Niu and Qingshu Yang contributed equally to this work.

Responsible editor: Hongwen Sun

✉ Lixia Niu
niulixia@mail.sysu.edu.cn

1 Institute of Estuarine and Coastal Research, School of Marine Engineering and Technology, Sun Yat-sen University, Guangzhou 510275, People's Republic of China

2 Guangdong Provincial Engineering Research Centre of Coasts, Islands and Reefs, Guangzhou 510006, People's Republic of China

3 Southern Laboratory of Ocean Science and Engineering, Zhuhai 519000, People's Republic of China

4 Section of Safety and Security Science, Delft University of Technology, 2628, BX Delft, the Netherlands

regions. They are characterized by strong gradients of factors such as salinity, as well as inorganic and organic pollutants as a result of riverine input and sewage outfalls (Timoney and Lee 2011; Liu et al. 2014, 2017). PAHs in aquatic environment are a key to controlling the ecological risks posed by such chemicals in water and sediments. Because of the low vapor pressures of PAHs, compounds with five or more rings exist mainly adsorbed to particulate matter, such as fly ash and soot, while those with four or fewer rings will occur both in the dissolved phase and adsorbed to particles (Chen et al. 2004; Liu et al. 2012). Therefore, PAHs in estuarine sediments can serve as effective tracers of materials transported from river-to-sea (Hu et al. 2014). Estuaries play a critical role in the transportation and fate of PAHs. Thus, investigations of PAHs in estuarine sediments can provide useful information for further understanding of environmental processes and transport of contaminants.

The contamination sources of PAHs are mainly in the form of incomplete combustion and petroleum leakage, which are largely attributed to anthropogenic activities (Zakaria et al. 2002; Zhang et al. 2012; Liu et al. 2017). Different anthropogenic sources and their contribution to the total PAHs lead to different types of PAH compound and composition (Yunker et al. 1996), which behave differently in the aquatic environment. PAHs can originate from natural processes such as biomass burning, volcanic eruptions, and diagenesis (Wang et al. 2007). PAHs are always emitted as a mixture of individual compounds, and the relative molecular concentrations are considered to be correlated with given emission sources (Tobiszewski and Namiesnik 2012).

The Pearl River Estuary (PRE), as our case zone, is one of the heavily urbanized or industrialized regions in the world. The increasing development activities in the Pearl River Delta have resulted in a large volume of wastewater entering into the PRE. Previous studies have extensively detected the PAHs in water samples and suspended particulate matter of the PRE due to anthropogenic impacts, e.g., the PAH depth profile (Yang et al. 2008), PAH distribution (Mai et al. 2003; Yuan et al. 2015), PAH composition (Liu et al. 2014, 2017), and PAH source (Wang et al. 2007; Liu et al. 2017). However, not much is known about the sources and environmental fate of sediment PAHs in the PRE. Based on a 1-year field survey conducted monthly in the PRE in 2011, the objectives of this study were (1) to study the estuarine behaviors of 62 sediment PAHs (e.g., distribution and composition); (2) to quantify the environmental correlations of sediment PAHs, especially the roles of sediment particles and total organic carbon (TOC); and (3) to distinguish the potential risk sources of sediment PAHs associated with anthropogenic pressures.

Materials and methods

Study area

The Pearl River Estuary (PRE), South China, is particularly known for the strong interactions between seawater tides and freshwater outflow. The source/sink exchange has increased the complexity of the PRE and has played an essential role in sediment PAHs. The PRE is characterized as a highly eutrophicated zone in China, packed with high concentrations of pollutants (e.g., PAHs, heavy metals, and nutrients). The system consists of three major tributaries, the East River, North River, and West River, as illustrated in Fig. 1. The freshwater discharges into the South China Sea via eight river gates (Humen, Jiaomen, Hongqili, Hengmen, Hutiaomen, Jitimen, Yamen, and Modaomen). The South China Sea becomes a receptor and contributes to global pollution via air-water exchange. There are substantial variations in hydrological conditions between the wet (April–September) and dry (October–March) seasons (Lu et al. 2009). Approximately 80% of the total annual freshwater outflow is discharged during the wet season (Zhao 1990).

The sampling site of the Humen outlet is located at the top of the PRE. Compared with the other seven river outlets, the Humen outlet is the most representative for investigating the abundance of PAHs (Liu et al. 2014, 2017; Niu et al. 2018). The Humen outlet is a tide-dominated channel. The behaviors of PAHs in this area are more complicated due to the strong interactions of riverine runoff and tidal currents. This outlet is also the main passage for the transport of pollutants from the cities of Guangzhou, Foshan, and Dongguan. Additionally, it is an important pool of the key processes from both the river networks (East River and North River) and Lingdingyang Bay.

Sample collection and sample analysis

Surface sediment samples (depth < 5 cm; two samples) were continuously obtained each month in 2011 (January 19, February 19, March 20, April 20, May 19, June 17, July 16, August 14, September 14, October 22, November 11, and December 19) using traditional active sampling in the Humen estuary. The sediment samples (a total of 24) were collected using a stainless steel grab sampler and were scooped into polyethylene sealed bags, shipped back to the laboratory, and stored at − 20 °C until further analysis. Salinity, temperature, and water depth were measured in situ using a conductivity-temperature-depth (CTD) SBE 19plus device. Precipitation data and freshwater discharge were derived from the Water Resources Department of Guangdong Province, accessible from http://www.gdwater.gov.cn/.

Sampling analysis was performed using a gas chromatograph (Agilent 6890, USA) interfaced with a mass

Fig. 1 Sketch map of the Pearl River Estuary (South China), and sampling site (22°48.622'N, 113°36.670'E) in the Humen outlet

spectrometer (Agilent 5973, USA) for GC-MS analysis. The extraction of PAHs was processed in an extraction cell with an accelerated solvent extractor (ASE), according to the EPA-3545A method. The solid samples were freeze-dried. Approximately 10-g solid sediment samples were mixed with pelletized diatomaceous earth and then loaded into the extraction cell, and surrogate standards were appended. The extraction solvent was prepared as a mixture of acetone/dichloromethane (V:V = 1:1). The solid samples were extracted for 10 min at 100 °C and 1500 psi in the extraction cell. Subsequently, the extraction was concentrated, solvent was exchanged with n-hexane, and the volume was further reduced to approximately 1 mL under weak nitrogen. The achieved extract was transferred to a 1:2 alumina/silica gel glass column for fractionation and cleanup.

All sediment samples were analyzed for 62 types of PAHs, namely, 2-ring PAHs (naphthalene (*Nap*), 2-methylnaphthalene, 1-methylnaphthalene, biphenyl, 2-ethylnaphthalene, 1-ethylnaphthalene, 2,6-dimethyl naphthalene, 1,3-dimethyl naphthalene, 2,3-dimethyl naphthalene, 1,5-dimethyl naphthalene, 1,2-dimethyl naphthalene, 1,8-dimethyl naphthalene, 2-methyl biphenyl, 3-methyl biphenyl, 4-methyl biphenyl, 2,2'-dimethyl biphenyl, 2-isopropylnaphthalene, 1,4,5-

trimethylnaphthalene, 2,3,5-trimethylnaphthalene, 3,3'-dimethyl biphenyl, and 4,4'-dimethyl biphenyl); 3-ring PAHs (dibenzofuran, acenaphthylene (*Aye*), acenaphthene (*Ace*), fluorene (*Flu*), 1-methyl fluorene, phenanthrene (*Phe*), anthracene (*Ant*), dibenzothiophene, 2-methyl phenanthrene, 3-methyl phenanthrene, 2-methyl anthracene, 1-methyl phenanthrene, 9-methyl anthracene, 2-ethyl anthracene, 3,6-dimethyl phenanthene, 9,10-dimethyl anthracene, and 1-methyl-7-isopropyl-phenanthene (retene)); 4-ring PAHs (fluoranthene (*Fluo*), pyrene (*Pyr*), benzo[b]naphtho[23-d]furan, 7,12-dimethyl-benzo[a]anthracene, 7-methyl benzo[a]anthracene, 1-methyl chrysene, 4-methyl chrysene, 2-methyl chrysene, benzo[c]phenanthrene, benzo[a]anthracene (*BaAn*), and chrysene (*Chr*)); 5-ring PAHs (benzo[ghi]fluoranthene, cyclopenta[cd]pyrene, benzo[b]fluoranthene (*BbFl*), benzo[k]fluoranthene (*BkFl*), benzo[a]fluoranthene, benzo[a]pyrene (*BaPy*), benzo[e]pyrene, and perylene, dibenzo[a,h]anthracene (*DiAn*), benzo[b]chrysene); and 6-ring PAHs (indeno[123-cd]fluoranthene, benzo[g,h,i]perylene (*BePe*), and indeno[123-cd]pyrene (*InPy*)). Of these, the *Nap*, *Aye*, *Ace*, *Flu*, *Phe*, *Ant*, *Fluo*, *Pyr*, *BaAn*, *Chr*, *BbFl*, *BkFl*, *BaPy*, *DiAn*, *BePe*, and *InPy* PAHs have been designated as 16 priority PAHs by the US EPA.

Quality assessment and quality control

Field blanks, laboratory blanks, and replicated samples were analyzed along with the field sediment samples. Concentrations of PAHs were corrected using the recoveries from surrogate standards (e.g., naphthalene-d_8, phenanthrene-d_{10}, fluoranthene-d_{10}, and pyrene-d_{10}). A 60 m × 0.25 mm-i.d. (0.25-μm film thickness) DB-5MS column (J&W Scientific, Folsom, CA, USA) was used for separating the target analytes. The GC column temperature was programmed to fall from 120 °C to 100 °C at a rate of 25 °C min^{-1} and then ramped up at a rate of 5 °C min^{-1} to 300 °C. Extract injection was conducted in the splitless mode with a split time of 5 min. The injection port, ion trap, manifold, and transfer line temperatures were maintained at 310, 190, 40, and 280 °C, respectively. Mass fragments were generated in the positive electron impact mode at an electron voltage of 70 eV and scanned from 50 to 300 amu. Recovery studies were performed to characterize the quality of the analytical methods. Limit of detection (LOD), recovery, and relative standard deviation were used for method assessment. The LOD for PAHs was 10 ng/g, and blanks were below the LOD.

As for the 16 priority PAHs in the surface sediments, the recoveries were 116.7±12.6% (*Nap*), 117.5±3% (*Aye*), 119±3.9% (*Ace*), 105.8±5.7% (*Flu*), 112±6.5% (*Phe*), 112±4.9% (*Ant*), 110±6.1% (*Fluo*), 108.1±1.8% (*Pyr*), 70±12.9% (*BeAn*), 107.2±1.8% (*Chr*), 72.8±8.8% (*BeFl*), 64.2±3.2% (*BkFl*), 114.3±1.4% (*BaPy*), 104.6±1.5% (*BePe*), 118.1±4.3% (*InPy*), and 126±2.8% (*DiAn*).

Data analysis

The sums of 62 PAHs, 16 priority PAHs, and 28 parent PAHs were defined as $\sum_t$PAHs, $\sum_{16}$PAHs, and $\sum_p$PAHs, respectively. Principal component analysis (PCA), using varimax rotation with Kaiser normalization, was employed to identify the potential risk sources of sediment PAHs (Liu et al. 2014, 2017; Niu et al. 2018). Additionally, the diagnostic ratio was explored in the source apportionment of the PAHs (Yunker et al. 2002; Lima et al. 2005). Pearson correlation (significance level $p < 0.05$) was performed to supplementally explain the environmental impacts of sediment PAHs. Moreover, in order to take random effects into account, a probabilistic analysis was performed to provide insight into the dynamics of the sediment PAH levels. The Kolmogorov-Smirnov (K-S) test was utilized to determine the probability models, which were needed for prediction purposes. Origin 8.0 software was used to plot the experiment data.

Results

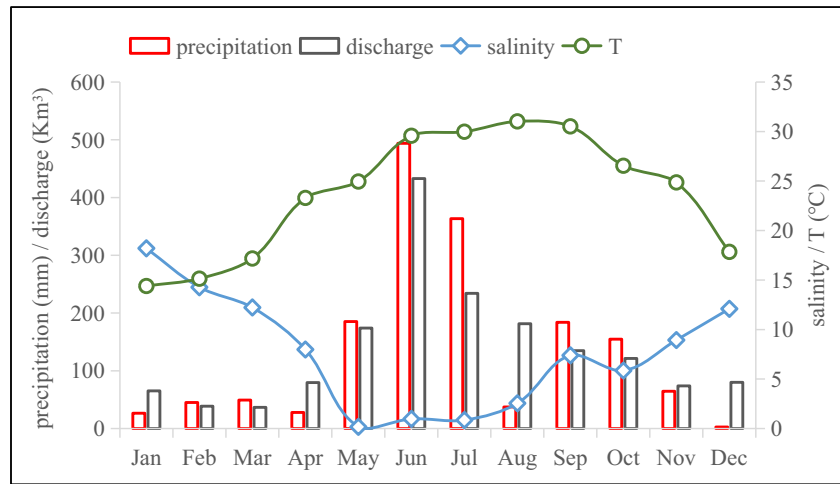### Seasonal variations in environmental properties

Hydrology. Hydrological cycles could be reflected in changes in the estuarine parameters, including SPM, salinity, and water temperature. The hydrological conditions (salinity, precipitation, freshwater discharge, and water temperature) during the sampling period were displayed in Fig. 2. The observed estuarine parameters in the Humen river mouth show significant seasonal variations. In 2011, the monthly mean velocity varied from 0.17 to 0.55 m/s. Salinity ranged from 0.17‰ to 18.21‰, and the mean salinity in the wet season was lower than that in the dry season. The riverine discharge was controlled by the precipitation, and approximately 80% of the annual precipitation concentrated during the wet season (April–September). The monthly water discharge ranged from 36.69 Km^3 (March) to 432.86 Km^3 (June), with a mean value of 137.75 Km^3. The mean temperature varied from 14.4 °C to 31.0 °C, and the mean water temperature in the wet season was higher than that in the dry season.

Suspended sediment (SPM) and total organic carbon (TOC). The monthly mean SPM ranged from 0.05 g/L to 0.31 g/L, with a mean value of 0.17 g/L. The monthly mean SPM in the wet season (0.21 g/L) was higher than that in the dry season (0.13 g/L). The seasonal variations of sediment properties (e.g., grain size, composition, and total organic carbon) are listed in Table 1. The mean value of grain size (Φ) varied from 4.75 to 7.20 mm, and the median size fell between 3.13 and 7.44 mm. The TOC content ranged from 6.34 to 11.42%, with a maximum in February and a minimum in October. The sediment property showed a less temporal pattern. The surface sediments throughout all the year (excluding October, November, and December) were predominantly composed of clayed sand, with the exception of silty sand in February. Silty clay was the main sediment composition in October and November, and sandy clay was dominant in December.

Seasonal variations in PAH levels

More than 62 types of PAHs in the surface sediments were detected each month in 2011. The summary statistics of total PAHs ($\sum_t$PAHs, $\sum_p$PAHs, and $\sum_{16}$PAHs) are shown in Fig. 3a. The concentration of $\sum_t$PAHs varied widely among the 12 months, from 0.835 to 2.753 μg/g, with a mean value of 1.517 μg/g and a standard deviation of 0.530 μg/g. The $\sum_t$PAHs peaked in February, while their minimum appeared in August. Of the 62 individual PAHs, perylene was the most abundant, accounting for 25% of the total PAHs concentrations. The correlations between total PAHs and naphthalene and pyrene were significant ($p < 0.05$), with respective correlation coefficients defined as 0.58 and 0.91. Twenty-eight

Fig. 2 Seasonal variations in salinity, precipitation, freshwater discharge, and water temperature in the Humen outlet during the sampling period

parent PAHs ($\sum_p$PAHs), accounting for 72% of the total, varied from 0.569 to 1.897 μg/g, with a mean value of 1.092 μg/g and a standard deviation of 0.379 μg/g. As for the 16 individual priority PAHs (Fig. 3b), naphthalene and pyrene, accounting for almost one-half (43.43%) of the total, were the predominant PAH compounds. The maximum concentration of naphthalene was found in January (0.447 μg/g), while the minimum concentration occurred in December (0.042 μg/g). It was noted that the naphthalene outliers mostly appeared in the dry season, while the concentrations in the flood season were relatively stable. Naphthalene was the predominant PAH compound, accounting for 31% of the $\sum_{16}$PAHs. The relative relationship of the mean values of the 16 individual priority PAHs was *Nap > Pyr > Fluo > Phe > BeFl > Chr > BaPy > InPy > Flu > BkFl > BeAn > Ant > DiAn > BePe > Ace > Aye*. Without naphthalene, the 15 remaining priority PAHs ($\sum_{15}$PAHs) ranged from 0.272 to 0.753 μg/g, with a mean

value of 0.404 μg/g. The $\sum_{16}$PAHs accounted for 39% of the $\sum_t$PAHs and ranged from 0.325 to 1.098 μg/g.

The flood and dry season characteristics are shown in Fig. 4. A small difference was found in the seasonal variation of the $\sum_{16}$PAHs (a mean of 0.52 μg/g for the flood season and a mean of 0.66 μg/g for the dry season). A moderate difference was found in the mean value of the $\sum_p$PAHs between the two seasons, 0.90 μg/g and 1.28 μg/g, respectively, while a large difference in the mean value of the $\sum_t$PAHs was found, 7.69 μg/g versus 10.51 μg/g, respectively. The mean value of the $\sum_t$PAHs during the flood season was lower than that during the dry season.
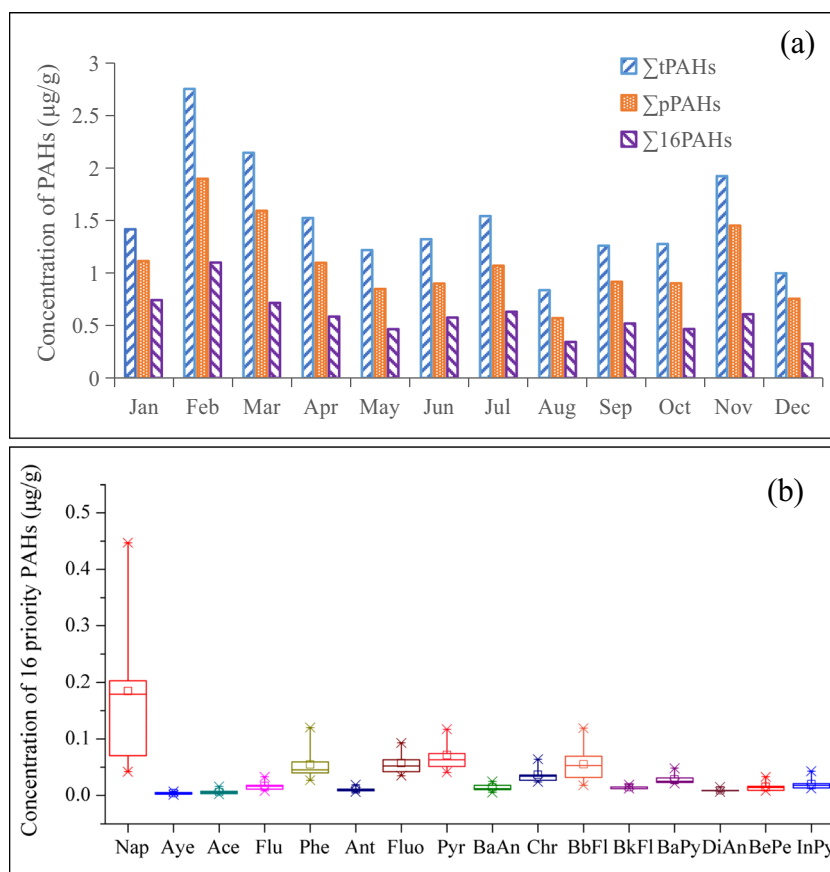
Seasonal assessment of PAH composition

Based on the number of aromatic rings, the PAHs were divided into two groups: low-molecular-weight PAHs (LMW-
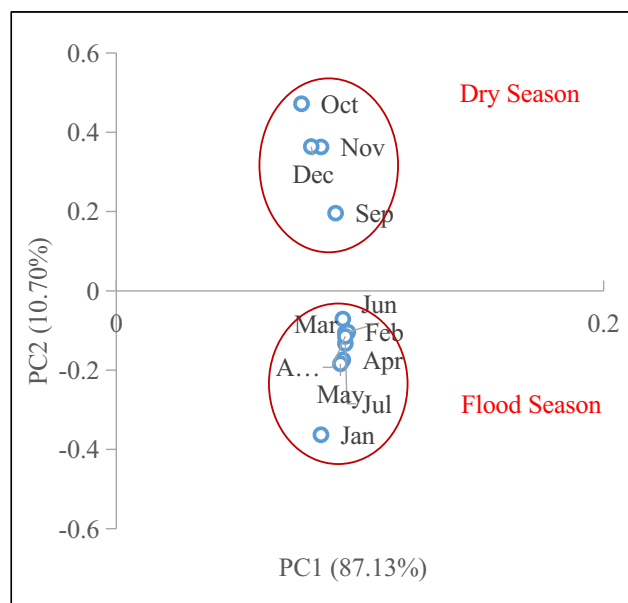
Table 1 Seasonal variations of sediment properties (e.g., suspended sediment, grain size, particle composition, and total organic carbon) in the Humen estuary in 2011

	SPM (g/L)	TOC (%)	Grain size (Φ, mm)		Sediment composition (%)		
			Mean size	Median size	Sand	Silt	Clay
Jan	0.067	9.97	4.75	3.15	57.93	19.10	22.97
Feb	0.088	11.42	4.92	3.13	57.86	18.40	23.74
Mar	0.211	9.87	4.83	3.14	58.57	22.78	18.65
Apr	0.312	8.18	5.27	3.81	51.57	22.18	26.24
May	0.129	7.77	6.37	6.3	42.50	23.69	33.81
Jun	0.214	7.45	5.14	3.23	54.46	19.14	26.40
Jul	0.298	7.84	5.55	4.39	48.46	22.00	29.53
Aug	0.113	6.64	5.12	3.23	54.12	20.24	25.63
Sep	0.177	7.67	6.38	6.06	44.12	22.52	33.36
Oct	0.234	6.34	7.20	7.44	20.91	37.49	41.60
Nov	0.108	9.28	6.93	7.41	23.21	34.42	42.37
Dec	0.053	7.57	6.45	7.08	32.67	21.95	45.39

Fig. 3 Seasonal variations of total PAHs ($\sum_t$PAHs, $\sum_p$PAHs, and $\sum_{16}$PAHs) in sediments of the Humen estuary in 2011 (a) and the boxplot of 16 individual priority PAHs (b)

Fig. 4 Principal component analysis for the monthly variation of the 16 individual polycyclic aromatic hydrocarbons in the surface sediments of the Humen outlet in 2011

PAHs) containing two or three aromatic rings and high-molecular-weight PAHs (HMW-PAHs) containing four to six aromatic rings. Figure 5 is a plot of the percentage of
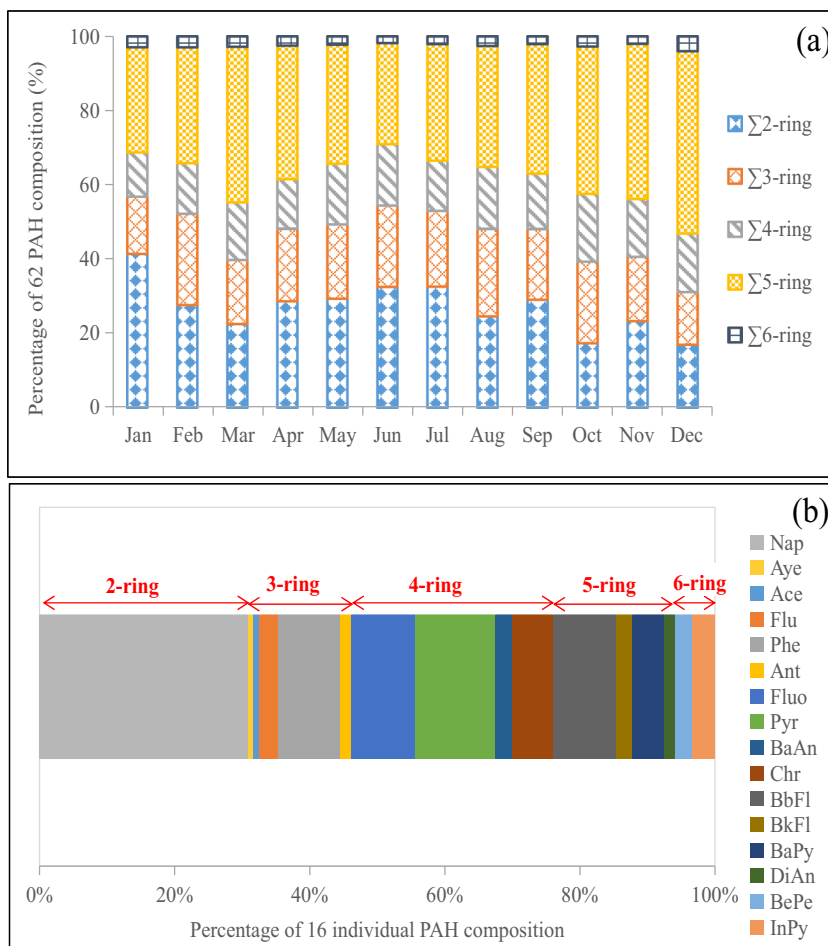
PAH compositions. The monthly mean values of $\sum$2-ring, $\sum$3-ring, $\sum$4-ring, $\sum$5-ring, and $\sum$5-ring PAHs were 0.41 µg/g, 0.30 µg/g, 0.23 µg/g, 0.54 µg/g, and 0.04 µg/g, respectively. The PAHs with five aromatic rings ($\sum$5-ring PAHs, e.g., perylene) were the most abundant PAH compounds, ranging from 0.27 to 0.90 µg/g and accounting for 27–49% of the $\sum_t$PAHs, implying that the potential source was from the terrestrial inputs via the Pearl River (Yuan et al. 2015). The abundances of $\sum$2-ring and $\sum$3-ring PAHs were followed, ranging from 0.17 to 0.76 µg/g and 0.14 to 0.67 µg/g, and accounting for 11–35% and 14.19–24.51% of the total, respectively. The levels of $\sum$4-ring PAHs ranged from 0.14 to 0.37 µg/g and accounted for 11.9–18.1% of the total. And the $\sum$6-ring PAHs varied from 0.02 to 0.08 µg/g and accounted for 1.8–2.9%.

Total LMW-PAHs (2-ring and 3-ring) ranged from 0.31 to 1.43 µg/g, with a mean value of 0.71 µg/g and a standard deviation of 0.28 µg/g. Their maximum occurred in February, while their minimum was in December. The concentration of total LMW-PAHs in the dry season (4.69 µg/g) was higher than that in the flood season (3.88 µg/g). The trend of total LMW-PAHs was similar to that of the total 16 priority PAHs. Total HMW-PAHs varied from 0.43–1.32 µg/g, with a mean value of 0.80 µg/g. The concentration of total HMW-PAHs in the dry season (5.81 µg/g) was higher than that in the

Fig. 5 Seasonal variations in percent of the 62 PAH compositions (**a**) and the 16 individual PAH compositions (**b**) in surface sediments of the Humen estuary in 2011

flood season (3.81 μg/g). For the total 62 PAHs ($\sum_t$PAHs), the HMW-PAHs were more prevalent than the LMW-PAHs.

Discussion

A comparison of sediment PAHs

The status of PAH contamination found in this study was compared with those in other estuaries, bays, and seas in China (Table 2). The mean concentrations of $\sum_{16}$PAHs in the Humen estuary were relatively higher than that reported for the Yangtze River Estuary (Li et al. 2012), Yellow River Estuary (Hu et al. 2014), Pearl River Estuary (Luo et al. 2005; Yuan et al. 2015), Daya Bay (Yuan et al. 2015), northern South China Sea (Yuan et al. 2015), Bohai Sea (Li et al. 2015), Yellow Sea (Li et al. 2015), and Luan River Estuary (Zhang et al. 2016). The levels of PAHs in this study were lower than detected in Pearl River Estuary by Luo et al. (2005). Comparison results suggested that the sediment PAHs in the Humen estuary were heavily polluted, which was consistent with the findings of Yuan et al. (2015). Therefore, the PAH contamination in this study ranked very high in China.

Hydrological effect

The concentration of PAHs varied throughout the sampling year, which may be due to the cumulative effects of environmental variables, e.g., tidal currents, the sedimentary rate of PAHs, the composition of sediments, and salinity. Table 3 lists the Pearson correlations between sediment PAHs and velocity, salinity, precipitation, fresh water discharge, and ambient water temperature. The velocity may promote the resuspension process and decrease the concentration of sediment PAHs. Thus, a negative relationship between sediment PAHs and velocity was found in which $\sum$4-ring and $\sum$5-ring PAHs were moderately correlated with the bottom velocity, with the correlation coefficient defining both being − 0.30. The contribution of salinity was positively significant in this case (r = 0.24–0.67), particularly for the HMW-PAHs (e.g., $\sum$5-ring and $\sum$6-ring), corresponding well with other studies (Jing et al. 2014). A negative correlation between PAHs and temperature was detected, as previously determined by Jensen and Hites (1983). Changes in temperature can affect the amount of total PAHs; specifically, higher temperatures favored the amount of total parent PAH compounds ($r = -0.59$). Temperature can also improve the adsorption of PAHs onto

Table 2 Comparison of sediment polycyclic aromatic hydrocarbons (PAHs; expressed in µg/g) examined in this study and adjacent zones (N indicates the number of sediment PAH compounds)

Location	N	Range	Mean	Sample year	Study
Humen estuary	62	0.835–2.753	1.517	2011	This study
Humen estuary	16	0.325–1.098	0.589	2011	This study
Yangtze River Estuary	16	0.090–0.502	0.221	2010	Li et al. 2012
Yellow River Estuary	16	0.097–0.204	0.152	2007	Hu et al.,2014
Pearl River Estuary	60	0.346–2.089	1.139	2011	Yuan et al. 2015
Pearl River Estuary	16	0.144–1.289	0.43	2011	Yuan et al. 2015
Pearl River Estuary	16	0.191–0.622	0.321	2002	Luo et al. 2005
Pearl River Estuary	16	0.217–2.680	1.028	2002	Luo et al. 2005
Pearl River Estuary	59	0.255–16.67	–	2002	Luo et al. 2005
Daya Bay	60	0.336–0.848	0.633	2011	Yuan et al. 2015
Daya Bay	16	0.140–0.491	0.310	2011	Yuan et al. 2015
Northern South China Sea	60	0.583–0.706	0.644	2011	Yuan et al. 2015
Northern South China Sea	16	0.274–0.335	0.304	2011	Yuan et al. 2015
Macao coast	48	0.294–12.74	–	1999	Mai et al. 2003
Bohai Sea	16	0.149–1.211	0.507	–	Li et al. 2015
Yellow Sea	16	0.148–0.907	0.548	–	Li et al. 2015
East China Sea	34	0.297–1.643	0.708	2010	Deng et al. 2013
Luan River Estuary	16	0.005–0.545	0.121	–	Zhang et al. 2016
Guan River estuary	21	0.09–0.218	0.132	2011	He et al. 2014

particles. The HMW-PAHs were greatly influenced by temperature, with correlation coefficients of -0.54 and -0.78 for $\sum$5-ring PAHs and $\sum$6-ring PAHs, respectively. As found with temperature, freshwater discharge also negatively contributed to sediment PAHs due to the riverine input. No significant correlation between precipitation and sediment PAHs was found in this study, although precipitation plays a role in the sedimentary rate of atmospheric PAHs (Lima et al. 2005). These results suggested that the sediments were heavily contaminated during the dry season, an occurrence that was closely related to the cumulative effects of the hydrodynamic conditions, e.g., salinity, temperature, and water discharge. Moreover, the strong interactions of tides and runoff as well as precipitation during the flood season greatly influenced the accumulation of PAHs in the surface sediments.

Influence of suspended particle

Sediment is an important pool of PAHs and can induce the secondary pollution of PAHs to the aquatic environment as a result of strong hydrodynamic conditions (Yang et al. 2008). The grain size of sediment particles can directly influence the

Table 3 Pearson correlation between sediment PAHs and environmental factors (salinity, velocity, and temperature measured at 0.5 m above the riverbed) as well as precipitation and fresh water discharge in the Humen outlet in 2011 (r is the Pearson correlation coefficient; p is the significance level)

PAHs	Velocity		Salinity		Precipitation		Discharge		T	
	r	p	r	p	r	p	r	p	r	p
$\sum$2-ring	0.20	0.53	0.39	0.22	0.03	0.92	-0.19	0.56	-0.47	0.12
$\sum$3-ring	-0.04	0.90	0.24	0.45	-0.04	0.91	-0.24	0.45	-0.35	0.26
$\sum$4-ring	-0.30	0.35	0.32	0.31	-0.09	0.78	-0.33	0.29	-0.41	0.18
$\sum$5-ring	-0.30	0.35	0.51	0.09	-0.35	0.26	-0.59	0.04	-0.54	0.07
$\sum$6-ring	-0.11	0.73	0.67	0.02	-0.44	0.15	-0.61	0.03	-0.78	0.00
$\sum_t$PAHs	-0.11	0.75	0.45	0.14	-0.16	0.61	-0.41	0.18	-0.53	0.08
$\sum_p$PAHs	-0.14	0.65	0.53	0.07	-0.23	0.47	-0.48	0.11	-0.59	0.04
$\sum_{16}$PAHs	0.04	0.90	0.47	0.12	-0.06	0.84	-0.29	0.36	-0.55	0.07

composition and distribution of PAHs in the environment (Lima et al. 2005; Li et al. 2019). In order to analyze the contributions of particle sizes, Pearson correlations were calculated between PAH composition and percentage of sediment fractions. Results showed that the concentration of total PAHs ($\sum_t$PAHs) was correlated with clay ($r = 0.60$) and the concentration of LMW-PAHs (e.g., $\sum$2-ring) was strongly correlated with sand ($r = 0.74$), as discussed by Allen et al. (1996). Sediment PAHs showed a higher tendency to be adsorbed onto the large-sized particles rather than the fine fractions due to particle properties and hydrodynamic conditions. Sediment TOC is a controlling factor for PAH behaviors, e.g., adsorption and environmental fate (Yan et al. 2016). In this study, the concentration of PAHs in surface sediments was found to be positively correlated with TOC content using a linear model ($r = 0.83$–0.95, $p < 0.01$), as displayed in Fig. 6. The concentration of $\sum$3-ring PAHs was highly linked to the TOC content ($r = 0.95$), followed in terms of correlation by $\sum$4-ring PAHs ($r = 0.88$), $\sum$5-ring PAHs ($r = 0.86$), $\sum$2-ring PAHs ($r = 0.84$), and $\sum$6-ring PAHs ($r = 0.83$). In addition, the contents of total organic carbon (TOC) may considerably facilitate the sediment PAH concentrations during the dry season (Gu et al. 2016).

The monthly concentrations of suspended particulate matter (SPM) displayed an obvious seasonal pattern due to the effects of hydrological cycles (Liu et al. 2017). A significant correlation was revealed between the sediment PAHs and suspended sediment load (Fig. 6), with correlation coefficients of 0.88, 0.93, 0.62, 0.86, and 0.84 for $\sum$2-ring, $\sum$3-ring, $\sum$4-ring, $\sum$5-ring, and $\sum$6-ring PAHs during the flood season, and 0.40, 0.72, 0.75, 0.27, and 0.16 during the dry season, respectively. PAHs with five or more aromatic rings preferentially adsorb onto sediment particles, while those with four or fewer rings would probably exist in the dissolved phase and particulate phase due to water solubility (Yuan et al. 2015; Gu et al. 2016; Liu et al. 2017). A higher concentration of suspended sediment was associated with a higher concentration of PAHs owing to adsorption (Sun and Zang 2013). The PAHs in the water column could accumulate in sediments via particle deposition, and the PAHs in sediments could possibly enter the water body through the resuspension process and pore water (Yang et al. 2008; Liu et al. 2012).
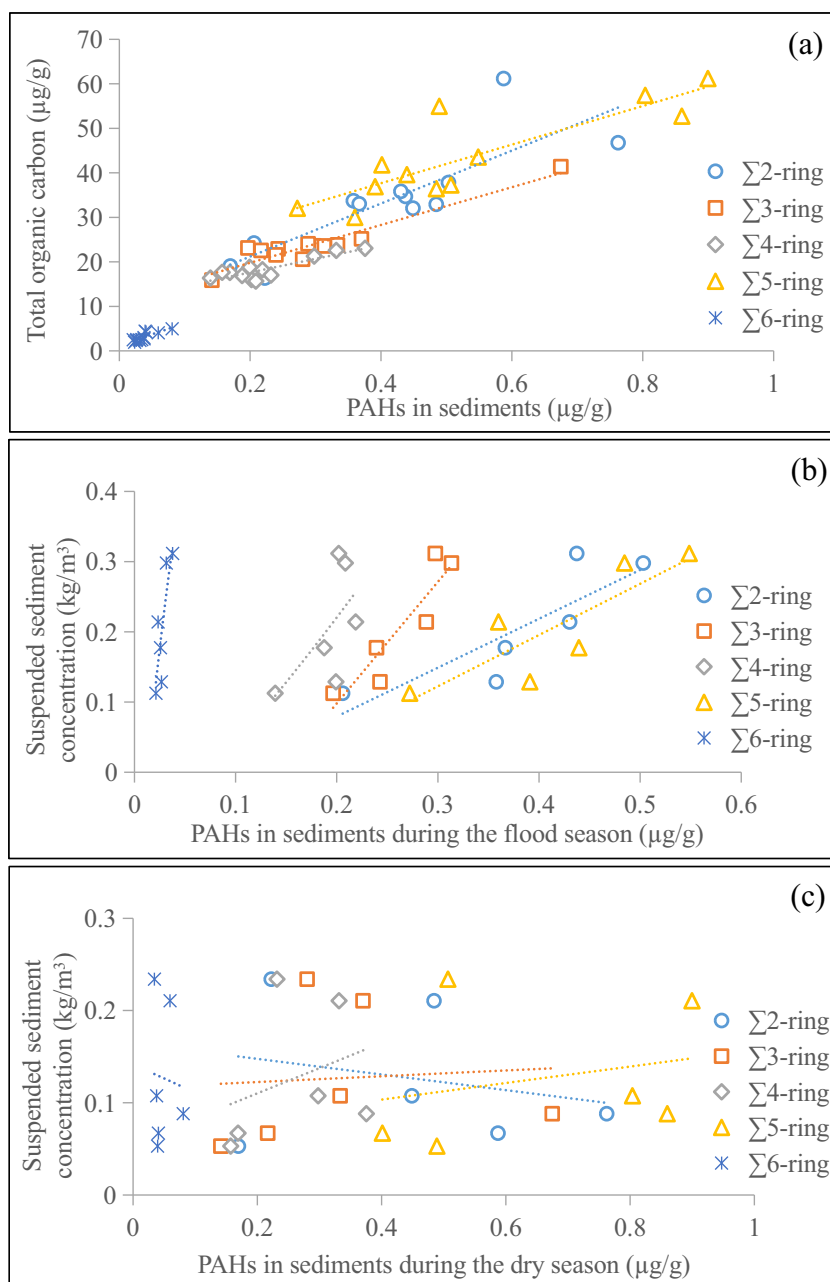
Source identification

A statistically based method, principal component analysis (PCA) was performed to explore the similarities and differences among 16 individual PAHs in the sediments of the Humen outlet in 2011. Based on the monthly variation of 16 individual PAHs, two principal components (PC1 and PC2) were identified via the criterion of eigenvalue > 1, with eigenvalues of 10.46 and 1.28, accounting for 87.13% and 10.70% of the total variance, respectively (see Fig. 4). The seasonal pattern was obvious, corresponding well with the hydrological cycles (e.g., precipitation, water discharge, and salinity).

The abundances of $\sum$2-ring and $\sum$3-ring PAHs further suggested that the sediment PAHs were transported via various pathways, e.g., atmospheric deposition and riverine discharge. The potential risk sources of PAHs originated mainly from incomplete combustion and petroleum leakage (e.g., wood burning, coke combustion, forest burning, petroleum pollution, and oil spills). In order to identify the contamination sources of the PAHs in the sediments, PCA using varimax rotation with Kaiser normalization was performed on the 62 individual PAHs in the environment, as listed in Table 4. The number of components corresponded to the number of variables (62). The seven original principal components (PC1, PC2, PC3, PC4, PC5, PC6, and PC7) were extracted to represent the total variance via the criterion of eigenvalue > 1, accounting for 97.17%. Moreover, the first component was more correlated with other factors than the second component. Figure 7 is the target diagram of the first 2 components of the 62 individual PAHs in the surface sediments of the Humen outlet in 2011.
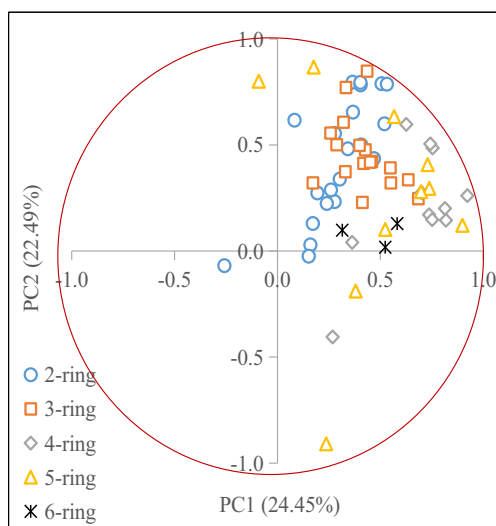
The first principal component PC1, with an eigenvalue of 41.32 and accounting for 24.45% of the total variance, was dominated by 4-ring PAHs (e.g., 4-methyl chrysene) and 5-ring PAHs (e.g., perylene). Larsen and Baker (2003) reported using HMW-PAHs (e.g., perylene, benzo[ghi]perylene, and indeno[123-cd]pyrene) as indicators of vehicle emissions. Thus, PC1 was identified as a vehicle emission source. PC2, with an eigenvalue of 7.30 and accounting for 22.49% of the total variance, was heavily weighted by 5-ring PAHs (e.g., benzo[k]fluoranthene). Benzo[k]fluoranthene is considered to be a tracer of diesel vehicles (Venkataraman and Friedlander 1994). Thus, PC2 was identified as a diesel vehicle source. PC3, with an eigenvalue of 3.89 and accounting for 22.13% of the total variance, was highly weighted by 2-ring PAHs (e.g., 2-methylnaphthalene). Tolosa et al. (1996) demonstrated that petroleum-derived residues included abundant LMW-PAHs (2- and 3-ring PAHs). Thus, PC3 was considered to be a petroleum source. PC4 and PC5, with eigenvalues of 2.95 and 2.27 and responsible for 18.85% and 4.27% of the total variance, respectively, were predominated by LMW PAHs (e.g., 1-methyl fluorene, 1,4,5-trimethylnaphthalene, and 1,8-dimethyl naphthalene). It has been determined that oil-fired power generation stations are characterized by 2-ring and 3-ring PAHs, specifically methylnaphthalenes and phenanthrene (Masclet et al. 1986). Thus, PC4 and PC5 were identified as oil combustion sources. PC6, with an eigenvalue of 1.40 and accounting for 2.57% of the total variance, was heavily weighted by 2-methyl anthracene. Fluoranthene, pyrene, phenanthrene, and anthracene have been flagged as coal combustion sources (Larsen and Baker 2003). Therefore, PC6 was identified as coal combustion. PC7 was responsible 2.41% of the total variance and was dominated by 3-ring

Fig. 6 Scatter plots of sediment
PAH composition versus total
organic carbon and suspended
sediment load (0.5 m above the
riverbed) in the Humen outlet in
2011

Table 4 Eigenvalues and total variance of 62 individual PAHs from principal component analysis

Component	Eigenvalue	Extraction sums of squared loadings		Rotation sums of squared loadings	
		% of variance	Cumulative %	% of variance	Cumulative %
PC1	41.32	66.65	66.65	24.45	24.45
PC2	7.30	11.77	78.42	22.49	46.94
PC3	3.89	6.28	84.70	22.13	69.08
PC4	2.95	4.75	89.45	18.85	87.92
PC5	2.27	3.66	93.11	4.27	92.19
PC6	1.40	2.26	95.37	2.57	94.76
PC7	1.12	1.80	97.17	2.41	97.17

Fig. 7 Target diagram of the first two components of the 62 individual PAHs in the surface sediments of the Humen outlet in 2011
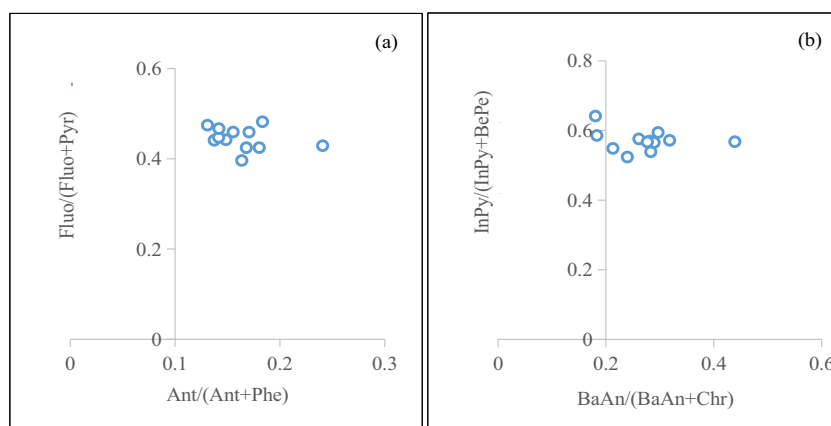
PAHs (e.g., retene). The presence of retene is used as a marker of wood combustion (Ramdahl 1983). Hence, PC7 was indicated as a wood combustion source. In summary, vehicle sources, petroleum sources, and combustion sources were identified as the major anthropogenic PAH contamination sources.

Additionally, diagnostic ratios of various individual PAHs have been used extensively to characterize the potential risk sources of PAHs (Yunker et al. 2002; Lima et al. 2005; Deng et al. 2013; Gu et al. 2016). In this study, the isomer ratios of Ant/(Ant+Phe) against Fluo/(Fluo+Pyr), and BaAn/(BaAn+Chr) against InPy/(InPy+BePe) were designed as indicators to assess the PAH input sources (Yunker et al. 2002; Martins et al. 2010), as depicted in Fig. 8. The ratios of Ant/(Ant+Phe) and InPy/(InPy+BePe) suggested the main PAH source was

from combustion (wood burning and coal burning), while the ratios of Fluo/(Fluo+Pyr) and BaAn/(BaAn+Chr) suggested the PAH source could be attributed to a mixture of combustion and petroleum leakage.
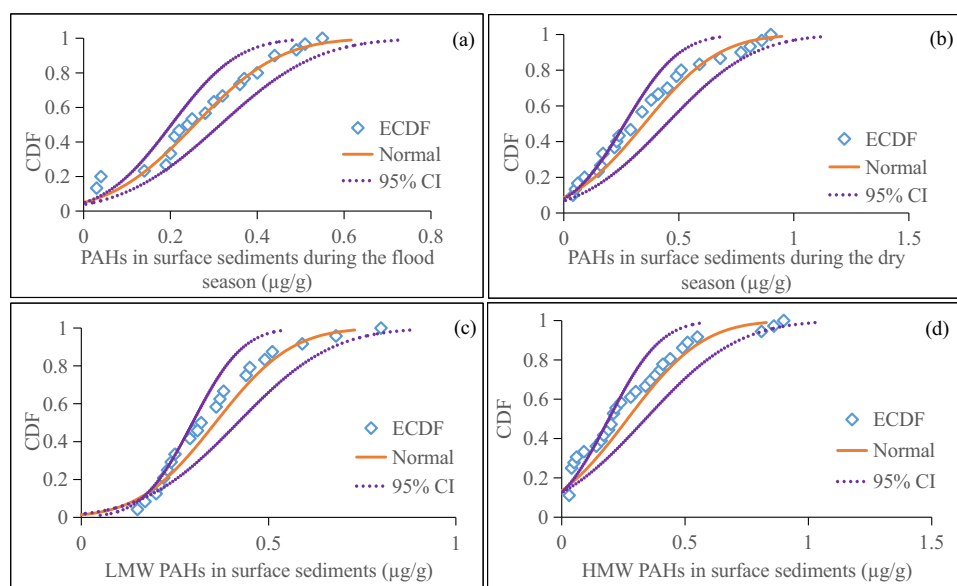
Probabilistic assessment

In the presence of random effects, originating from sampling errors and experimental errors, a probability analysis was required to provide insights into the reliable range of sediment PAHs in the Humen outlet. The frequency distribution of PAHs demonstrated that there were no obvious extremes or outliers in the dataset. Most of the concentrations were clustered in the center. The widely used Kolmogorov-Smirnov (K-S) test implied that the empirical cumulative density function (ECDF) of PAHs in surface sediments was fitted well by the cumulative density function (CDF) of the preferred normal distribution (see Fig. 9). During the flood season, a normal distribution with 0.256 ± 0.155 µg/g was determined to predict more than 90% of sediment PAHs within the 95% confidence interval (CI), while a normal distribution with 0.35 ± 0.257 µg/g may predict 95% of the sediment PAHs during the dry season. The ECDF of LMW-PAHs in surface sediments was moderately fitted with the CDF of the preferred normal distribution (0.358 ± 0.160 µg/g) within the 95% CI (lower 2.5% bound, 0.297 ± 0.106 µg/g; upper 97.5% bound, 0.418 ± 0.198 µg/g), while the ECDF of HMW-PAHs agreed considerably with the CDF of the preferred normal distribution (0.267 ± 0.242 µg/g, lower 2.5% bound, 0.191 ± 0.166 µg/g; upper 97.5% bound, 0.340 ± 0.296 µg/g). A nondeterministic method was utilized

Fig. 8 Potential input sources of PAHs in sediments from the Humen outlet in 2011. A value of Ant/(Ant+Phe) < 0.1 indicated the PAH input source was from petroleum emissions, while a value > 0.1 implied a combustion source (e.g., grass, wood, or coal). A value of Fluo/(Fluo+Pyr) < 0.4 indicated the source was from petroleum emissions and a value > 0.5 implied a combustion source, while a value between 0.4 and 0.5

indicated petroleum combustion. A value of InPy/(InPy+BePe) < 0.2 indicated the PAH source was from petroleum emissions, and a value >0.5 implied the main source was combustion, while a value between 0.2 and 0.5 implied petroleum combustion. A value of BaAn/(BaAn+Chr) < 0.2 indicated the main source was from petroleum emissions, while a value > 0.35 implied a combustion source (Yunker et al. 2002)

Fig. 9 Probabilistic assessment of sediment PAHs in the Humen outlet in 2011 at a specific significance level of 95% (**a**, flood season; **b**, dry season; **c**, LMW-PAHs; **d**, HMW-PAHs)

Conclusions

The estuarine dynamics of sediment PAHs in the Pearl River Estuary were explored in this study, thereby helping to fill the knowledge gap of this complex region and providing valuable information for estuarine management. The estuarine PAH patterns in surface sediments varied widely throughout the sampling year. Perylene (5-ring PAHs) was the most abundant PAH compound, followed by the abundances of ∑2-ring and ∑3-ring PAHs, which implied various pathways for PAH transportation, e.g., a terrestrial input source via the Pearl River, adsorption onto particles, and atmospheric deposition. Significant correlations were examined between sediment PAHs and TOC as well as suspended sediment load. It was found that TOC could facilitate sediment PAHs and was a controlling factor for PAH behaviors. The surface sediments were predominantly composed of clayed sand. Moreover, sediment PAHs demonstrated a greater tendency to be adsorbed onto coarse particles rather than fine fractions due to particle properties and hydrodynamic conditions. The PCA results suggested that vehicle emission sources, petroleum sources, coal combustion, and wood combustion were the major human contamination sources of sediment PAHs. A deeper understanding of sediment PAH patterns is still needed, including the effects of physicochemical properties and human activities.

in this study to provide insight into the analyses of estuarine PAHs with random effects, which presented the reliable range at a specific significance level.

Compliance with ethical standards

Conflict of interest The authors declare no competing financial interest.

References

Allen JO, Dookeran NM, Smith KA, Sarofim AF, Taghizadeh K, Lafleur AL (1996) Measurement of polycyclic aromatic hydrocarbons associated with size-segregated atmospheric aerosols in Massachusetts. Environ Sci Technol 30:1023–1031

Cetin B (2016) Investigation of PAHs, PCBs and PCNs in soils around a heavily industrialized area in Kocaeli, Turkey: concentrations, distributions, sources and toxicological effects. Sci Total Environ 560-561:160–169

Chen B, Xuan X, Zhu L, Wang J, Gao Y, Yang K, Shen X, Lou B (2004) Distributions of polycyclic aromatic hydrocarbons in surface waters, sediments and soils of Hangzhou City, China. Water Res 38:3558–3568

Deng W, Li XG, Li SY, Ma YY, Zhang DH (2013) Source apportionment of polycyclic aromatic hydrocarbons in surface sediment of mud areas in the East China Sea using diagnostic ratios and factor analysis. Mar Pollut Bull 70:266–273

Gu Y, Ke C, Liu Q, Lin Q (2016) Polycyclic aromatic hydrocarbons (PAHs) in sediments of Zhelin Bay, the largest mariculture base on the eastern Guangdong coast, South China: characterization and risk implications. Mar Pollut Bull 110:603–608

Harrison RM, Smith DJT, Luhana L (1996) Source apportionment of atmospheric polycyclic aromatic hydrocarbons collected from an

urban location in Birmingham, UK. Environ Sci Technol 30:825–832

He XR, Pang Y, Song XJ, Chen BL, Feng ZH, Ma YQ (2014) Distribution, sources and ecological risk assessment of PAHs in surface sediments from Guan River Estuary, China. Mar Pollut Bull 80:52–58

Hu N, Huang P, Liu J, Ma D, Shi X, Mao J, Liu Y (2014) Characterization and source apportionment of polycyclic aromatic hydrocarbons (PAHs) in sediments in the Yellow River estuary, China. Environ Earth Sci 71:873–883

Jensen TE, Hites RA (1983) Aromatic diesel emissions as a function of engine conditions. Anal Chem 55:594–599

Jing L, Chen B, Zhang B, Zheng J, Liu B (2014) Naphthalene degradation in seawater by UV irradiation: the effects of fluence rate, salinity, temperature and initial concentration. Mar Pollut Bull 81:149–156

Kannan K, Johnson-Restrepo B, Yohn SS, Giesy JP, Long DT (2005) Spatial and temporal distribution of polycyclic aromatic hydrocarbons in sediments from Michigan inland lakes. Environ Sci Technol 39:4700–4706

Lang C, Tao S, Liu W, Zhang Y, Simonich S (2008) Atmospheric transport and outflow of polycyclic aromatic hydrocarbons from China. Environ Sci Technol 42:5196–5201

Larsen RK, Baker JE (2003) Source apportionment of polycyclic aromatic hydrocarbons in the urban atmosphere: a comparison of three methods. Environ Sci Technol 37:1873–1881

Li B, Feng C, Li X, Chen Y, Niu J, Shen Z (2012) Spatial distribution and source apportionment of PAHs in surficial sediments of the Yangtze estuary, China. Mar Pollut Bull 64:636–643

Li J, Dong H, Zhang D, Han B, Zhu C, Liu S, Liu X, Ma Q, Li X (2015) Sources and ecological risk assessment of PAHs in surface sediments from Bohai Sea and northern part of the Yellow Sea, China. Mar Pollut Bull 96:485–490

Li Y, Wang G, Wang J, Jia Z, Zhou Y, Wang C, Yanyan L, Zhou S (2019) Determination of influencing factors on historical concentration variations of PAHs in West Taihu Lake, China. Environ Pollut 249:573–580

Lima ALC, Farrington JW, Reddy CM (2005) Combustion-derived polycyclic aromatic hydrocarbons in the environment-a review. Environ Forensic 6:109–131

Liu L, Wang J, Wei G, Guan Y, Zeng EY (2012) Polycyclic aromatic hydrocarbons (PAHs) in continental shelf sediment of China: implications for anthropogenic influences on coastal marine environment. Environ Pollut 167:155–162

Liu F, Yang Q, Hu Y, Du H, Yuan F (2014) Distribution and transportation of polycyclic aromatic hydrocarbons (PAHs) at the Humen river mouth in the Pearl River delta and their influencing factors. Mar Pollut Bull 84:401–410

Liu F, Niu L, Chen H, Li P, Tian F, Yang Q (2017) Seasonal changes of polycyclic aromatic hydrocarbons in response to hydrology and anthropogenic activities in the Pearl River Estuary, China. Mar Pollut Bull 117:255–263

Lu F, Ni H, Liu F, Zeng EY (2009) Occurrence of nutrients in riverine runoff of the Pearl River Delta, South China. J Hydrol 376:107–115. https://doi.org/10.1016/j.jhydrol.2009.07.018

Luo X, Chen S, Mai B, Zeng Y, Sheng G, Fu J (2005) Distribution and sources of polycyclic aromatic hydrocarbons in sediments from rivers of Pearl River Delta and its nearby South China Sea. Environ Sci 26:129–134

Mai B, Qi S, Zeng EY, Yang Q, Zhang G, Fu J, Sheng G, Peng P, Wang Z (2003) Distribution of polycyclic aromatic hydrocarbons in the coastal region off Macao, China: assessment of input sources and transport pathways using compositional analysis. Environ Sci Technol 37:4855–4863

Martins CC, Bicego MC, Rose NL, Taniguchi S, Lourenco RA, Figueira RC, Mahiques MM, Montone RC (2010) Historical record of polycyclic aromatic hydrocarbons (PAHs) and spheroidal carbonaceous particles (SCPs) in marine sediment cores from Admiralty Bay, King George Island, Antarctica. Environ Pollut 158:192–200

Masclet P, Mouvier G, Nikolaou K (1986) Relative decay index and sources of polycyclic aromatic hydrocarbons. Atmos Environ 20:439–446

Moeckel C, Monteith DT, Llewellyn NR, Henrys PA, Pereira MG (2014) Relationship between the concentrations of dissolved organic matter and polycyclic aromatic hydrocarbons in a typical U.K. upland stream. Environ Sci Technol 48:130–138

Niu L, Cai H, van Gelder PHAJM, Luo P, Liu F, Yang Q (2018) Dynamics of polycyclic aromatic hydrocarbons (PAHs) in water column of Pearl River estuary (China): seasonal pattern, environmental fate and source implication. Appl Geochem 90:39–49

Qiu YW, Zhang G, Liu GQ, Guo LL, Li XD, Wai O (2009) Polycyclic aromatic hydrocarbons (PAHs) in the water column and sediment core of Deep Bay, South China. Estuar Coast Shelf Sci 83:60–66

Ramdahl T (1983) Retene-a molecular marker of wood combustion in ambient air. Nature 306:580–582

Sun L, Zang S (2013) Relationship between polycyclic aromatic hydrocarbons (PAHs) and particle size in dated core sediments in Lake Lianhuan, Northeast China. Sci Total Environ 461-462:180–187

Timoney KP, Lee P (2011) Polycyclic aromatic hydrocarbons increase in Athabasca river delta sediment: temporal trends and environmental correlates. Environ Sci Technol 45:4278–4284

Tobiszewski M, Namiesnik J (2012) PAH diagnostic ratios for the identification of pollution emission sources. Environ Pollut 162:110–119

Tolosa I, Bayona JM, Albaigés J (1996) Aliphatic and polycyclic aromatic hydrocarbons and sulfur/oxygen derivatives in northwestern Mediterranean sediments: spatial and temporal variability, fluxes, and budgets. Environ Sci Technol 30:2495–2503

Usman M, Hanna K, Haderlein S (2016) Fenton oxidation to remediate PAHs in contaminated soils: a critical review of major limitations and counter-strategies. Sci Total Environ 569-570:179–190

Valavanidis A, Vlachogianni T, Triantafillaki S, Dassenakis M, Androutsos F, Scoullos M (2008) Polycyclic aromatic hydrocarbons in surface seawater and in indigenous mussels (Mytilus galloprovincialis) from coastal areas of the Saronikos Gulf (Greece). Estuar Coast Shelf Sci 79:733–739

Venkataraman C, Friedlander SK (1994) Size distribution of polycyclic aromatic hydrocarbons and elemental carbon. 2. Ambient measurement and effects of atmospheric processes. Environ Sci Technol 28:563–572

Wang J, Guan Y, Ni H, Luo X, Zeng EY (2007) Polycyclic aromatic hydrocarbons in riverine runoff of the Pearl River delta (China): concentrations, fluxes, and fate. Environ Sci Technol 41:5614–5619

Yan J, Liu J, Shi X, You X, Cao Z (2016) Polycyclic aromatic hydrocarbons (PAHs) in water from three estuaries of China: distribution, seasonal variations and ecological risk assessment. Mar Pollut Bull 109:471–479

Yang Q, Lei Y, Ou S, Mai B, Fu J, Sheng G (2008) Vertical distribution, composition of polycyclic aromatic hydrocarbons in water column from Guangzhou channel in the Pearl River. Mar Sci Bull 27:34–43

Yuan K, Wang X, Lin L, Zou S, Li Y, Yang Q, Luan T (2015) Characterizing the parent and alkyl polycyclic aromatic hydrocarbons in the Pearl River estuary, Daya Bay and northern South China Sea: influence of riverine input. Environ Pollut 199:66–72

Yunker MB, Snowdon LR, Macdonald RW, Smith JN, Fowler MG, Skibo DN, Mclaughlin FA, Danyushevskaya AI, Petrova VI, Ivanov GI (1996) Polycyclic aromatic hydrocarbon composition and potential sources for sediment samples from the Beaufort and Barents Seas. Environ Sci Technol 30:1310–1320

Yunker MB, Macdonald RW, Vingarzan R, Mitchell RH, Goyette D, Sylvestre S (2002) PAHs in the Fraser River basin: a critical appraisal of PAH ratios as indicators of PAH source and composition. Org Geochem 33:489–515

Zakaria MP, Takada H, Tsutsumi S, Ohno K, Yamada J, Kouno E, Kumata H (2002) Distribution of polycyclic aromatic hydrocarbons (PAHs) in rivers and estuaries in Malaysia: a widespread input of petrogenic PAHs. Environ Sci Technol 36:1907–1918

Zhang Y, Guo CS, Xu J, Tian YZ, Shi GL, Feng YC (2012) Potential source contributions and risk assessment of PAHs in sediments from Taihu Lake, China: comparison of three receptor models. Water Res 46:3065–3073

Zhang D, Liu J, Jiang X, Cao K, Yin P, Zhang X (2016) Distribution, sources and ecological risk assessment of PAHs in surface sediments from the Luan River Estuary, China. Mar Pollut Bull 102:223–229

Zhao H (1990) Evolution of the Pearl River Estuary. Ocean Press, Beijing